



OPEN ACCESS

EDITED BY

Wen-Zhou Zhang,
Xiamen University, China

REVIEWED BY

Kui Wang,
Zhejiang University, China
Zhibing Jiang,
Ministry of Natural Resources, China

*CORRESPONDENCE

Fajin Chen
✉ fjchen@gdou.edu.cn

RECEIVED 07 February 2024

ACCEPTED 18 March 2024

PUBLISHED 27 March 2024

CITATION

Chen C, Lao Q, Zhou X, Zhu Q and
Chen F (2024) Changes in hydrodynamics
and nutrient load of the coastal bay
induced by Typhoon Talim (2023).
Front. Mar. Sci. 11:1383528.
doi: 10.3389/fmars.2024.1383528

COPYRIGHT

© 2024 Chen, Lao, Zhou, Zhu and Chen. This is an open-access article distributed under the terms of the [Creative Commons Attribution License \(CC BY\)](https://creativecommons.org/licenses/by/4.0/). The use, distribution or reproduction in other forums is permitted, provided the original author(s) and the copyright owner(s) are credited and that the original publication in this journal is cited, in accordance with accepted academic practice. No use, distribution or reproduction is permitted which does not comply with these terms.

Changes in hydrodynamics and nutrient load of the coastal bay induced by Typhoon Talim (2023)

Chunqing Chen^{1,2}, Qibin Lao^{1,2}, Xin Zhou³, Qingmei Zhu^{1,2}
and Fajin Chen^{1,2,4*}

¹College of Ocean and Meteorology, Guangdong Ocean University, Zhanjiang, China, ²College of Chemistry and Environmental Science, Guangdong Ocean University, Zhanjiang, China, ³Institute of Marine Science, Shantou University, Shantou, China, ⁴Key Laboratory of Climate, Resources and Environment in Continental Shelf Sea and Deep Sea of Department of Education of Guangdong Province, Guangdong Ocean University, Zhanjiang, China

Typhoons can greatly alter the hydrodynamic and nutrient supply in coastal oceans. However, due to the complex conditions of typhoons, such as their intensity, even slight changes may cause substantial changes in hydrodynamics and nutrient supply, which needs to be better understood. In this study, we conducted two cruises before and after Typhoon Talim (2023) to quantitatively investigate changes in hydrodynamics and nutrient supply in Zhanjiang Bay using dual water isotopes. Before the typhoon, strong stratification occurred in the bay. However, the strong external force of the typhoon destroyed the stratification and substantially changed the water mixing in the bay after the typhoon. In the upper bay, massive freshwater input remarkably decreased the salinity during the post-typhoon period (freshwater increased by 18%). In contrast, the salinity variation in the lower bay was minimal, mainly due to massive seawater intrusion from the outer bay induced by the typhoon; the seawater mixed with freshwater columns from the upper bay, forming a strong ocean front. The intensity of ocean fronts induced by typhoons directly depended on the typhoon intensity landing in Zhanjiang Bay, as stronger typhoons will cause more intrusion of high-salinity seawater from the outer bay. Due to the formation of the ocean front, freshwater and terrestrial nutrients from the upper bay are prevented from being transported downwards, resulting in a large amount of accumulated pollutants within the bay. By contrast, due to the impact of high-salinity seawater intrusion, the contribution of seawater from the outer bay has increased, thereby diluting the nutrients in the lower bay. This study provides a new insight into the responses of coastal marine eco-environment systems to typhoons.

KEYWORDS

water isotopes, water masses, nutrient supply, ocean front, typhoons, Zhanjiang Bay

Introduction

Typhoons, also known as hurricanes and cyclones, are one of the most destructive extreme weather events that seriously disrupt human socioeconomic development. They can not only change the marine dynamics (Price, 1981; Liu et al., 2017; Doong et al., 2019), but also substantially impact the marine eco-environment (Shibano et al., 2011; Qiu et al., 2019; Zhou et al., 2021; Chen et al., 2023; Lao et al., 2023a). Particularly in the coastal waters, typhoons can increase the input of massive terrestrial nutrients, and can enhance water mixing to carry the deeper eutrophic water to the upper layer (Lao et al., 2023b; 2023c; Chen et al., 2024). These processes will lead to a series of marine ecological problems, such as algal blooms (Wang et al., 2016; Jiang et al., 2022; Li et al., 2022), decomposition of organic matter (Zhou et al., 2021; Lu et al., 2022; Lao et al., 2023a), hypoxia (Wang et al., 2017; Li et al., 2019; Zhao et al., 2021; Meng et al., 2022). Therefore, studying the changes in ocean hydrodynamic processes and nutrient supplies caused by typhoons will be beneficial for us in gaining a deeper understanding of their impact on the marine eco-environment.

Traditionally, the changes in water masses were studied by methods of hydrological parameters, satellite remote sensing, and numerical simulations (Bigg and Rohling, 2000; Lao et al., 2022a). Most of these methods based on observing changes in temperature and salinity, which are not attributes of water itself (Bigg and Rohling, 2000). Dual water isotopes (δD and $\delta^{18}O$) are considered as one of the best proxies for tracing past and modern ocean dynamics (Sengupta et al., 2013; Brady et al., 2019; Reyes-Macaya et al., 2022; Lao et al., 2022a). They are conservative tracers (Bigg and Rohling, 2000; Lian et al., 2016; Oshun et al., 2016), and their combination with hydrological parameters can effectively compensate for shortcomings of traditional methods. Even in the complex hydrodynamic coastal waters, they can quantify the mixing of different water masses and their impacts on the coastal eco-environment (Lao et al., 2022a; 2022b; Zhou et al., 2022; Chen et al., 2024).

Zhanjiang Bay, a semi-enclosed bay in the northwestern South China Sea (SCS), is directly or indirectly impacted by 10 typhoons every year (Chen et al., 2021), making it an ideal area for studying the response of ocean hydrodynamics and nutrient supplies to typhoons. It is a renowned aquaculture hub in China, with an annual export volume of seafood ranking among the top in China. Some extreme climate events, such as typhoons, can also cause seawater to intrude on coastal bays (Mori et al., 2014; Tanim and Goharian, 2021; Feng et al., 2023). In addition, typhoon events can increase terrestrial nutrient input into the bay due to increased runoff during the period (Lao et al., 2023c; Chen et al., 2024). These processes seriously threaten the eco-environment and aquaculture activities in Zhanjiang Bay (Zhou et al., 2021; Lao et al., 2023c; Chen et al., 2024). Under climate change, the intensity of typhoons is constantly increasing (Elsner et al., 2008; Balaguru et al., 2016; Zhou et al., 2019). Recently, dual water isotopes have been successfully applied to identify and quantify the hydrodynamic changes caused by typhoon events (Lao et al., 2023b, 2023c; Chen et al., 2024). However, due to the complexity of typhoon conditions, such as intensity, migration path, movement speed, rainfall, etc., these conditions can significantly alter hydrodynamic processes and

nutrient supplies. Under intensified typhoons, it is still unclear whether this will increase the amount of high-salinity seawater intrusion, thereby exacerbating the deterioration of water bodies in the bay and endangering local aquaculture activities. To address this issue, we present a new dataset of stable water isotopes, hydrological parameters and nutrients in the seawater of Zhanjiang Bay before and after Typhoon Talim (2023) to quantitatively study the changes in hydrodynamics and nutrient supply induced by the typhoon in the bay. This study will deepen our understanding of the response of the hydrodynamic and eco-environmental effects of coastal bays to typhoons.

Materials and methods

Study area and Typhoon Talim

Zhanjiang Bay is surrounded by Zhanjiang City (Figure 1). There is a Suixi River at the top of the upper bay. The annual runoff of the river is $10.4 \times 10^8 \text{ m}^3$, and it directly flows into the upper bay. The depth in the bay ranges from 2 to 23 m, with the lower bay being deeper. Only a narrow outlet (width of ~2 km) connects Zhanjiang Bay with the SCS water outside the bay (Figure 1). In the outer bay, a West-Guangdong Coastal Current (WGCC) affects Zhanjiang Bay year-round. During the summer, stronger coastal current can intrude the high-salinity seawater outside the bay into Zhanjiang Bay (Lao et al., 2022b). Affected by the East Asian monsoon, rainfall in the rainy seasons (April–October) (>85% of the annual rainfall) is much higher than in other seasons (Chen et al., 2019, 2021). Moreover, due to frequent typhoon events, the amount of rainfall brought by typhoons can reach over 50% of the annual rainfall in this region (Chen et al., 2021).

Typhoon Talim (2023) generated near the Luzon Island in July 14. It migrated northwest at an average speed of 4.3 m s^{-1} (a range of $1.7\text{--}6.1 \text{ m s}^{-1}$, from <https://typhoon.slt.zj.gov.cn/###>), passing through the SCS and increasing its intensity in the northwestern SCS (with maximum wind speed reaching 40 m s^{-1}) before making landfall in Zhanjiang Bay in July 17 (Figure 1A). Affected by Typhoon Talim, heavy rainfall occurred in Zhanjiang Bay during the typhoon period (with a rainfall of over 300 mm), with the highest rainfall (over 100 mm on July 18) occurring after the typhoon made landfall.

Field sampling

Two cruises were conducted in Zhanjiang Bay before (July 05) and two days after the Typhoon Talim landfall (July 19). Seven stations, including four in the upper bay and three in the lower bay, were established in each cruise (Figure 1B). In addition, during the typhoon period, five rainwater samples were collected on the roof of Guangdong Ocean University, located about 3 km from Zhanjiang Bay. Among them are two rainwater samples before the typhoon, and three rainwater samples during the typhoon period. Rainfall is recorded simultaneously during the collection of rainwater samples. Surface and bottom seawater

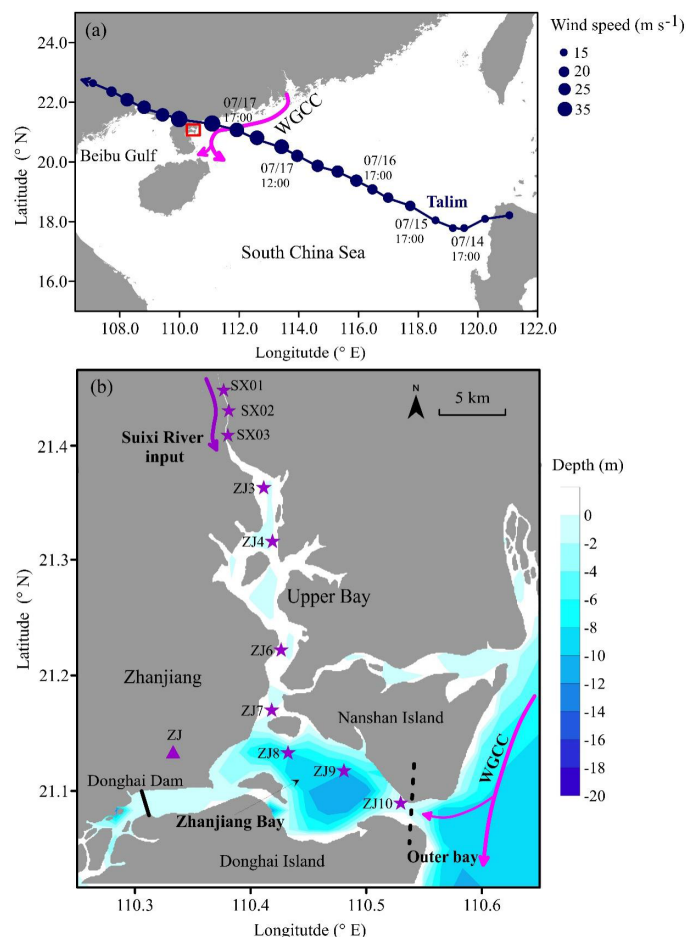


FIGURE 1

The track of Typhoon Talim (dark blue dotted line) (A) and the sampling stations (dark pink star) in Zhanjiang Bay (B). The red box in (A) is the study area. The dark pink triangle in Zhanjiang city is the location of rainwater sampling point. The three stations in the Suixi River were obtained from [Chen et al. \(2024\)](#). The pink arrows represent the West-Guangdong Coastal Current, which was modified from the study of [Lao et al., 2022b](#) and [2023c](#).

samples were collected using Niskin bottles (10 L) in each station before and after the typhoon cruises.

Seawater temperature, salinity and depth were determined on-site using an RBR Maestro multiparameter water quality monitor (RBRmaestro3, RBR, Canada). After sampling, about 1000 mL seawater was filtered by glass fiber filters (GF/F, 0.7 μm aperture and 47 mm diameter, Whatman) for the dual water isotope (δD and $\delta^{18}\text{O}$) and nutrient samples, and the filtrate was transferred into the pre-cleaned acid-washed polyethylene bottles. The pre-treatment process of dual water isotope in seawater samples followed the study of [Lao et al. \(2022a, 2022b, 2023b\)](#), and the rainfall samples followed the study of [Chen et al. \(2021\)](#).

Chemical analysis

Nutrient samples (NO_2^- , NO_3^- , PO_4^{3-} , and SiO_3^{2-}) were measured by a San++ continuous flow analyzer (Skalar, Netherlands), and the samples for NH_4^+ were measured using spectrophotometry. The measurements of δD and $\delta^{18}\text{O}$ followed the procedures prescribed by [Lao et al. \(2022a, 2023b\)](#) using an isotope ratio mass spectrometer

(Gasbench II-IRMS) (Gasbench II interfaced with a 253 plus mass spectrometer). H_2 and CO_2 were used to equilibrate δD and $\delta^{18}\text{O}$, and these equilibrated gases were measured using the Gasbench II-IRMS. For the measurement of δD , Pt catalyst was added into the 200 μL seawater sample, and a small amount of H_2 (2% H_2/He) was injected to make D/H in water and D/H in H_2 , to be in isotopic equilibrium at 28.00 $^\circ\text{C}$ for 40 min. For the measurement of $\delta^{18}\text{O}$, a small amount of CO_2 (1% CO_2/He) was injected into a 500 μL seawater sample to make $^{18}\text{O}/^{16}\text{O}$ in isotopic equilibrium at 24.00 $^\circ\text{C}$ for at least 24 hours. The international standard reference materials for water (VSMOW2, GISP, and SALP2) were used to calibrate the samples, and the precision for δD and $\delta^{18}\text{O}$ was $\pm 0.5\text{‰}$ and $\pm 0.1\text{‰}$, respectively. The detection limits for NO_2^- , NO_3^- , NH_4^+ , PO_4^{3-} , and SiO_3^{2-} were 0.1 $\mu\text{mol L}^{-1}$, 0.1 $\mu\text{mol L}^{-1}$, 0.1 $\mu\text{mol L}^{-1}$, 0.02 $\mu\text{mol L}^{-1}$ and 0.45 $\mu\text{mol L}^{-1}$, respectively.

Bayesian stable isotope mixing model

As the water isotopes are conserved and less affected by the water environment, the proportion of mixing between different

water masses can be quantified using the Bayesian model (Wu et al., 2021; Lao et al., 2022a, 2022b, 2023b, 2023c). The Bayesian model was constructed using the Stable Isotope Analysis software package in R (SIAR). The framework and detailed information on the Bayesian model were described by Lao et al. (2022a) and Moore and Semmens (2008). In this study, we first excluded the influence of water isotope fractionation after water mass mixing through the relationship between $\delta^{18}\text{O}$ and deuterium excess (*d*-excess, defined as $\delta\text{D} - 8 \times \delta^{18}\text{O}$, can be used as an indicator for kinetic fractionation, which exhibits an inverse relationship with $\delta^{18}\text{O}$ during evaporation) (Dansgaard, 1964). In this study, four end-members, including the fresh diluted water from the top of the upper bay, rainwater, groundwater around the Zhanjiang Bay and the seawater from the outer bay, were used to quantify the contribution of different water sources to the bay before and after the typhoon. The data on groundwater around Zhanjiang Bay was obtained from our previous study (Lao et al., 2022b). Due to the minor seasonal variation of δD and $\delta^{18}\text{O}$ in groundwater around the Zhanjiang Bay, the groundwater water end-member for the pre- and post-typhoon periods were all obtained from the study of Lao et al. (2022b). The rainwater end-member was obtained from the average values of δD and $\delta^{18}\text{O}$ in rainwater during the pre- and post-typhoon periods, respectively. The fresh diluted water end-member was obtained from the δD and $\delta^{18}\text{O}$ values in the Suixi River during summer (Chen et al., 2024), which is similar to the sampling period of this study. The seawater end-member was obtained from the station ZJ10. These end-member values are presented in Table 1.

Calculation of contribution of nutrients from different potential water sources

The mixing of water masses can alter the distribution of nutrients in the local marine environment (Lao et al., 2022a, 2023a; Chen et al., 2024). According to the proportional contribution of each water source and their nutrient concentrations, the contribution of the different water sources to the nutrient load in Zhanjiang Bay can be calculated by the follows:

$$Q_f = \frac{P_f \times C_f}{P_f \times C_f + P_o \times C_o + P_g \times C_g + P_r \times C_r} \text{ and} \quad (1)$$

$$Q_o = \frac{P_o \times C_o}{P_f \times C_f + P_o \times C_o + P_g \times C_g + P_r \times C_r} \text{ and} \quad (2)$$

$$Q_g = \frac{P_g \times C_g}{P_f \times C_f + P_o \times C_o + P_g \times C_g + P_r \times C_r} \text{ and} \quad (3)$$

$$Q_p = \frac{P_r \times C_r}{P_f \times C_f + P_o \times C_o + P_g \times C_g + P_r \times C_r} \text{ and} \quad (4)$$

where *Q* is the contribution of water masses to the nutrient load in Zhanjiang Bay (*f*: freshwater; *o*: outer bay; *g*: groundwater; *r*: rainwater), *P* is the contribution from each water source to the seawater of Zhanjiang Bay, and *C* is the nutrient concentrations of each water end-member (Table 2).

Statistical analysis

The Pearson's correlation analysis and Student's *t*-test analysis were conducted using SPSS Statistics 19.0. Before conducting the Pearson's correlation analysis and Student's *t*-test analysis, all variables were tested for normality using Kolmogorov-Smirnov test.

Results

Changes in hydrological characteristics after the typhoon

Before the typhoon, a high temperature (30.07–32.15°C) was observed in Zhanjiang Bay, especially in the surface water, and the temperature gradually decreased from the upper bay to the lower bay (Figure 2A). The salinity ranged from 16.4 to 30.7, and the lowest salinity was observed at the top of the upper bay, with a decreased trend toward the lower bay (Figure 2C). Higher temperature (an average of 31.35°C) but lower salinity (an average of 25.2) in the surface water than those in the bottom water (an average of 30.76°C for temperature and of 26.8 for salinity), suggesting that moderate stratification occurred in the water column of Zhanjiang Bay during the pre-typhoon period. However, the water temperature (28.03–30.03°C) and salinity (4.8–29.8) dropped remarkably after Typhoon Talim (Figure 2). Particularly in the upper bay, the surface water temperature dropped by 2.07°C during the post-typhoon period, indicating that strong external force of the typhoon has destroyed the stratification structure in the water column of the bay. In

TABLE 1 End-member values of potential water sources in Zhanjiang Bay.

Source	Pre-typhoon period		Post-typhoon period	
	$\delta^{18}\text{O}$ (‰)	δD (‰)	$\delta^{18}\text{O}$ (‰)	δD (‰)
Freshwater	-5.2 ± 0.0	-36.1 ± 3.8	-5.2 ± 0.0	-36.1 ± 3.8
Outer bay	-0.6 ± 0.1	-3.3 ± 1.2	-0.8 ± 0	-8.2 ± 1.8
Groundwater	-6.0 ± 0.8	-36.6 ± 4.6	-6.0 ± 0.8	-36.6 ± 4.6
Rainwater	-3.8 ± 0.5	-26.6 ± 5.3	-9.5 ± 3.1	-67.0 ± 25.9

TABLE 2 Nutrient concentrations ($\mu\text{mol L}^{-1}$) associated with each end-member in Zhanjiang Bay.

	Pre-typhoon					Post-typhoon				
	NO_3^-	NH_4^+	NO_2^-	PO_4^{3-}	SiO_3^{2-}	NO_3^-	NH_4^+	NO_2^-	PO_4^{3-}	SiO_3^{2-}
Freshwater	136.99	27.27	13.97	4.96	140.52	136.99	27.27	13.97	4.96	140.52
Outer bay	2.12	4.19	0.82	0.40	11.90	1.82	5.17	0.41	0.64	12.39
Groundwater	0.37	2.55	0.03	0.15	15.42	0.37	2.55	0.03	0.15	15.42
Rainwater	34.24	62.58	0.19	0.34	0.10	14.78	26.83	0.24	0.02	0.04

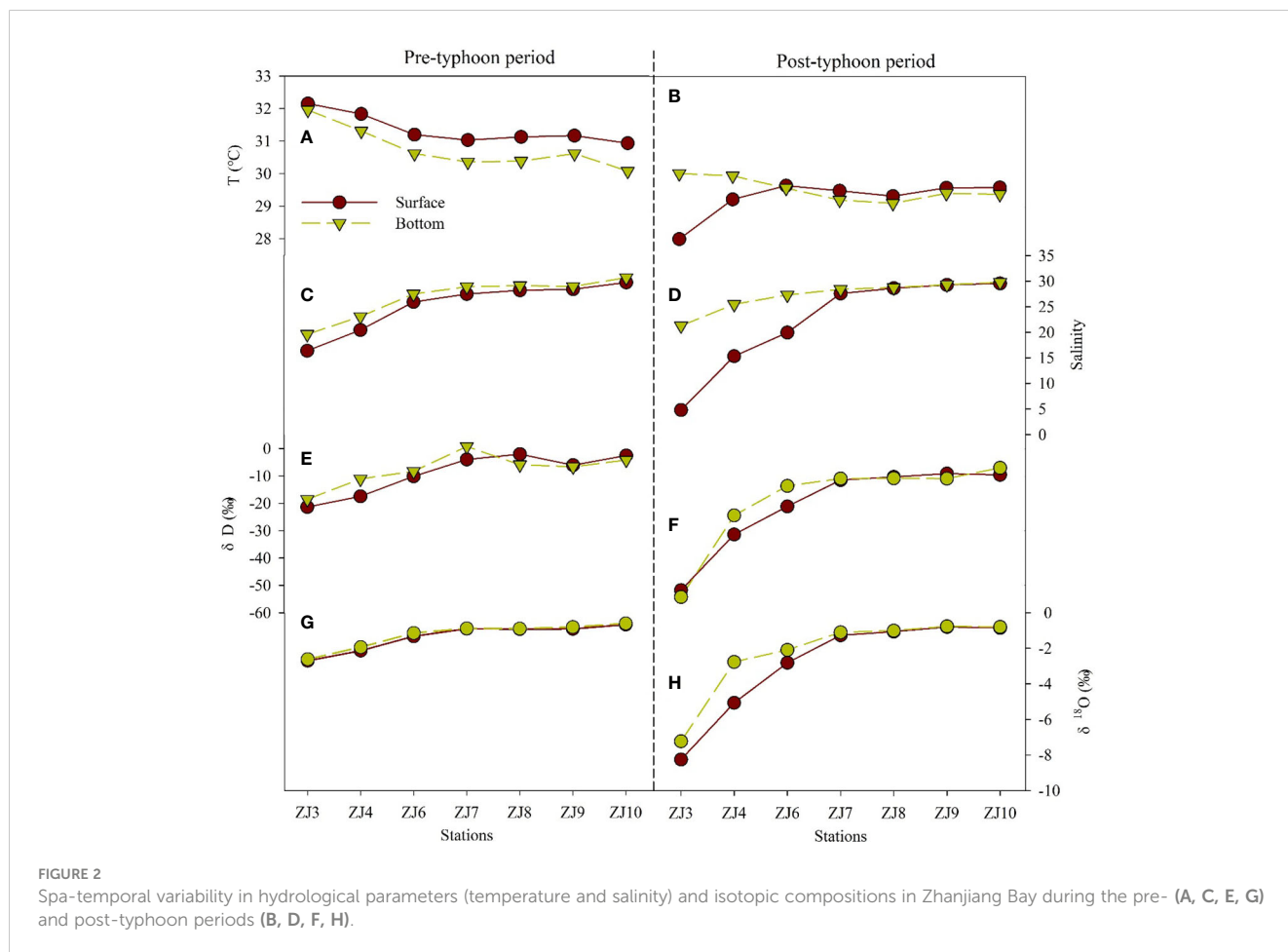
Nutrient end-members were consistent with water sources. The nutrient data from the freshwater and groundwater were obtained from Chen et al. (2024) and Lao et al. (2022b), respectively.

addition, the salinity in the upper bay has also decreased from an average of 22.6 during the pre-typhoon period to an average of 16.9 during the post-typhoon period. This indicated that the heavy rainfall during the typhoon period increased runoff input into the bay. However, the salinity in the lower bay exhibited less variation after the typhoon, with an average of 29.2 during both periods. Moreover, after the typhoon, the salinity in the surface water was almost consistent with the bottom water in the lower bay (Figure 2D), which was different from the distribution before the typhoon (average of 28.8 on the surface, an average of 29.6 on the bottom water). This indicated that in addition to the freshwater input and the stratification destroyed by the typhoon, the typhoon might cause intrusion of high-salinity water from the outer bay during the typhoon period. Remarkably, the surface salinity gradient increased substantially in the upper bay (from ZJ3 to

ZJ7, with ~ 22.0 km) after the typhoon (with a salinity gradient of 1.04 psu km^{-1} during the post-typhoon) (Figures 2C, D), which further indicates the intrusion of high-salinity seawater and the formation of a strong salinity front by mixing a large amount of freshwater input into the bay.

Changes in isotope compositions after the typhoon

Before the typhoon, δD and $\delta^{18}\text{O}$ values ranged from -21.4‰ to 0.8‰ and from -2.7‰ to -0.6‰ in the Zhanjiang Bay, with an average of -8.4‰ and -1.3‰ , respectively. Both δD and $\delta^{18}\text{O}$ values in the surface water was similar to the bottom water, and the values increased gradually from the upper bay to the lower bay (Figures 2E, G).



However, similar to the salinity, the δD and $\delta^{18}O$ values decreased remarkably and formed a large isotopic value gradient in the upper bay during the post-typhoon period (Figures 2F, H). δD and $\delta^{18}O$ values ranged from -54.4‰ to -7.0‰ and from -8.3‰ to -0.8‰ in the Zhanjiang Bay during the post-typhoon period, with an average of -19.7‰ and -2.6‰ , respectively. In the upper bay, δD and $\delta^{18}O$ values dropped substantially from the pre-typhoon period (an average of -13.2‰ for δD and -1.8‰ for $\delta^{18}O$) to the post-typhoon period (an average of -28.9‰ for δD and -4.4‰ for $\delta^{18}O$). However, a minor decrease in δD and $\delta^{18}O$ values was observed in the lower bay (an average of -3.5‰ for δD and -0.8‰ for $\delta^{18}O$ during the pre-typhoon, and an average of -9.6‰ for δD and -0.9‰ for $\delta^{18}O$). In the rainwater, the δD and $\delta^{18}O$ values ranged from -30.4‰ to -22.9‰ and from -4.2‰ to -3.4‰ during the pre-typhoon period. However, the values decreased substantially during the post-typhoon periods (from -96.9‰ to -50.0‰ for δD and from -13.2‰ to -7.4‰ for $\delta^{18}O$).

Changes in nutrient concentrations after the typhoon

Before the typhoon, the concentrations of NO_2^- , NO_3^- , NH_4^+ , PO_4^{3-} , and SiO_3^{2-} ranged from 0.6 to $5.2 \mu\text{mol L}^{-1}$, 1.6 to $46.6 \mu\text{mol L}^{-1}$, 3.9 to $21.0 \mu\text{mol L}^{-1}$, 0.3 to $4.1 \mu\text{mol L}^{-1}$ and 10.0 to $61.8 \mu\text{mol L}^{-1}$, respectively. They all exhibited higher concentrations at the top of the upper bay (station ZJ3), gradually decreasing toward the lower bay with increasing salinity. This indicated the influence of terrestrial nutrient input in the bay. In addition, there is no significant difference in nutrient concentration between the surface and bottom layers during the pre-typhoon period (t -test, $p > 0.05$). However, except for the NO_2^- , the nutrient concentrations increased remarkably in the bay during the post-typhoon period, particularly in the upper bay (Figure 3). After the typhoon, the concentrations of NO_2^- , NO_3^- , NH_4^+ , PO_4^{3-} , and SiO_3^{2-} ranged from 0.4 to $4.5 \mu\text{mol L}^{-1}$, 1.8 to $70.5 \mu\text{mol L}^{-1}$, 3.4 to $42.2 \mu\text{mol L}^{-1}$, 0.6 to $5.1 \mu\text{mol L}^{-1}$ and 11.5 to $61.3 \mu\text{mol L}^{-1}$, respectively. In the upper bay, the concentrations of NO_3^- , NH_4^+ , PO_4^{3-} , and SiO_3^{2-} during the post-typhoon period were 1.7 times, 1.9 times, 1.5 times, 1.3 times, respectively, higher than the pre-typhoon period (Table 3). However, in the lower bay, the nutrient concentrations were decreased during the post-typhoon period compared to the pre-typhoon period (except for PO_4^{3-}) (Table 3). This further indicated that the intrusion of high-salinity seawater from the outer bay has diluted the nutrients in the lower bay, while the formation of a salinity front in the upper bay caused by the typhoon has retained nutrients in the upper bay (the barrier effect of the front). In addition, the nutrient concentrations in the rainwater during the typhoon period were lower than those in the pre-typhoon period (Table 3), which could be related to the nutrients in the rainwater being diluted by the heavy rainfall during the typhoon period.

Relationships between the isotopic and salinity values with nutrient concentrations

The correlation between isotopic values and other physiochemical parameters is presented in Table 4. There was a

significantly positive relationship between δD and $\delta^{18}O$ values with salinity in Zhanjiang Bay during both pre- and post-typhoon periods, indicating that the seawater mixed well in the bay during these two periods. In addition, significantly negative relationships were found between the nutrient concentrations with salinity and dual water isotopic values during pre- and post-typhoon periods. This indicated that nutrient distribution was greatly influenced by water mixing in the bay.

Discussion

The typhoon induced massive high-salinity seawater intrusion into the bay

Correlations of δD - $\delta^{18}O$ and $\delta D/\delta^{18}O$ -salinity are commonly used to indicate the mixing processes of water masses, as their relationship changes after mixing with other water sources, such as precipitation, runoff, and large-scale ocean mixing (Kumar et al., 2018; Reyes-Macaya et al., 2022; Lao et al., 2023b, 2023c; Craig and Gordon, 1965; Lian et al., 2016; Chen et al., 2020). In nature, the change in D value (over 250%) is larger than that of ^{18}O because the variability in the abundance of δD is much higher than $\delta^{18}O$ (Dawson and Siegwolf, 2007). Therefore, after mixing with other water sources, the change in δD will be greater than in $\delta^{18}O$, resulting in changing their relationship (slope) (Lao et al., 2023c). For example, when seawater mixes with water that is characterized by lower isotopic values, such as runoff and precipitation, the slope of δD - $\delta^{18}O$ will increase; when the seawater mixes with water that is characterized by higher isotopic values such as high-salinity seawater and evaporation, the slope will decrease (Craig and Gordon, 1965; Lao et al., 2022a, 2022b; Deshpande et al., 2013; Kumar et al., 2018). Moreover, dual water isotopes and salinity have an empirical relationship, greatly affected by marine hydrology and dynamics (Lao et al., 2023b). Their linear relationships are expected to be modified after mixing with other water masses (Deshpande et al., 2013; Kumar et al., 2018).

In this study, the slope of δD - $\delta^{18}O$ (8.65) during the pre-typhoon period (Figure 4) was higher than the global meteoric water line (GMWL, 8.0) (Craig, 1961) and the global ocean water line (GOWL, 7.37) (Rohling, 2007), and it was close to the precipitation line (8.96) in the Zhanjiang Bay (Chen et al., 2021) and the seawater of northwestern SCS (outer Zhanjiang Bay, 8.64) during summer (Lao et al., 2023b). This suggested that the seawater in the bay during the pre-typhoon period could be influenced by the input of precipitation, which is related to the frequent heavy rainfall during that period (Lao et al., 2022b, 2023c). In addition, the slope of $\delta^{18}O$ -salinity (0.16) was lower than that in the Beibu Gulf (adjacent to Zhanjiang Bay, 0.25) during summer (Lao et al., 2022a), the SCS (0.27) during summer. This indicated that the seawater may also be influenced by the mixing with high-salinity water or evaporation, or both (Craig and Gordon, 1965; Rohling, 2007; Sengupta et al., 2013). The evaporation process can be excluded because of the decoupling relationship between d -excess and $\delta^{18}O$ before the typhoon (Figure 4B). Therefore, the intrusion of high-salinity could be responsible for the lower slope of $\delta^{18}O$ -salinity in the bay. Although the higher rainfall occurred in the

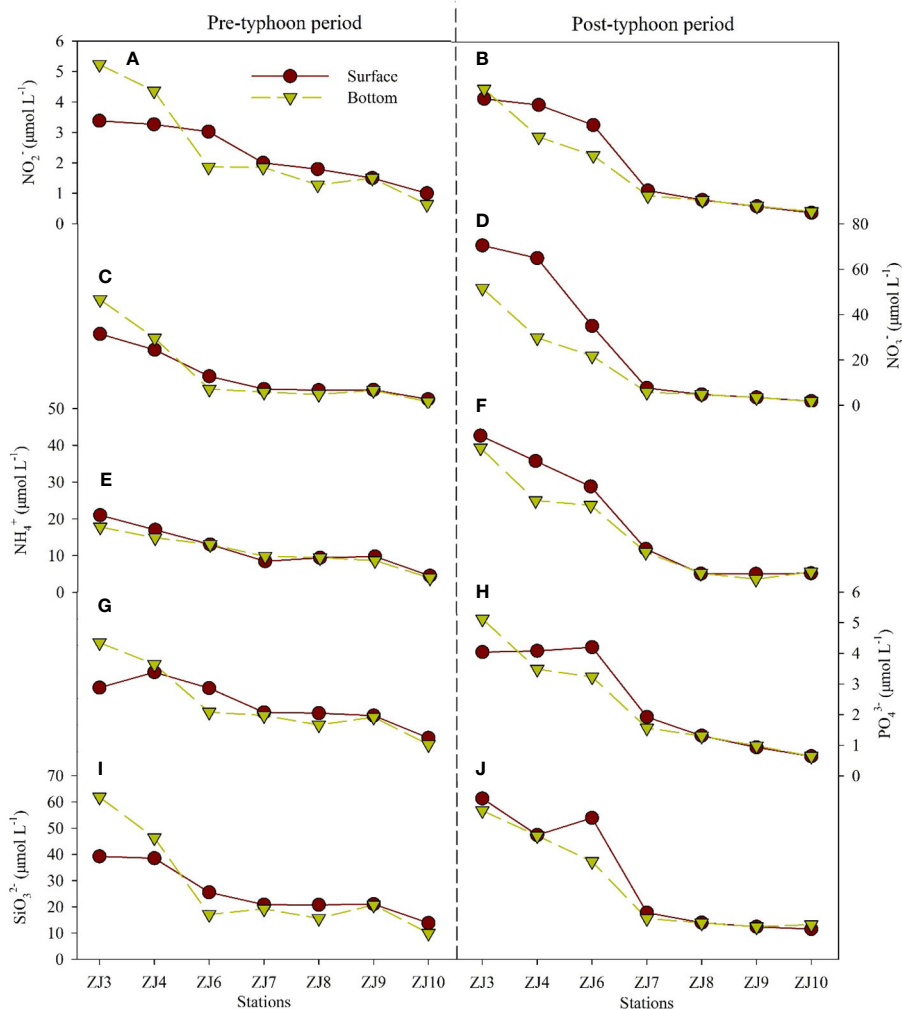


FIGURE 3 Spa-temporal variability in nutrient concentrations in Zhanjiang Bay during the pre- (A, C, E, G) and post-typhoon periods (B, D, F, H).

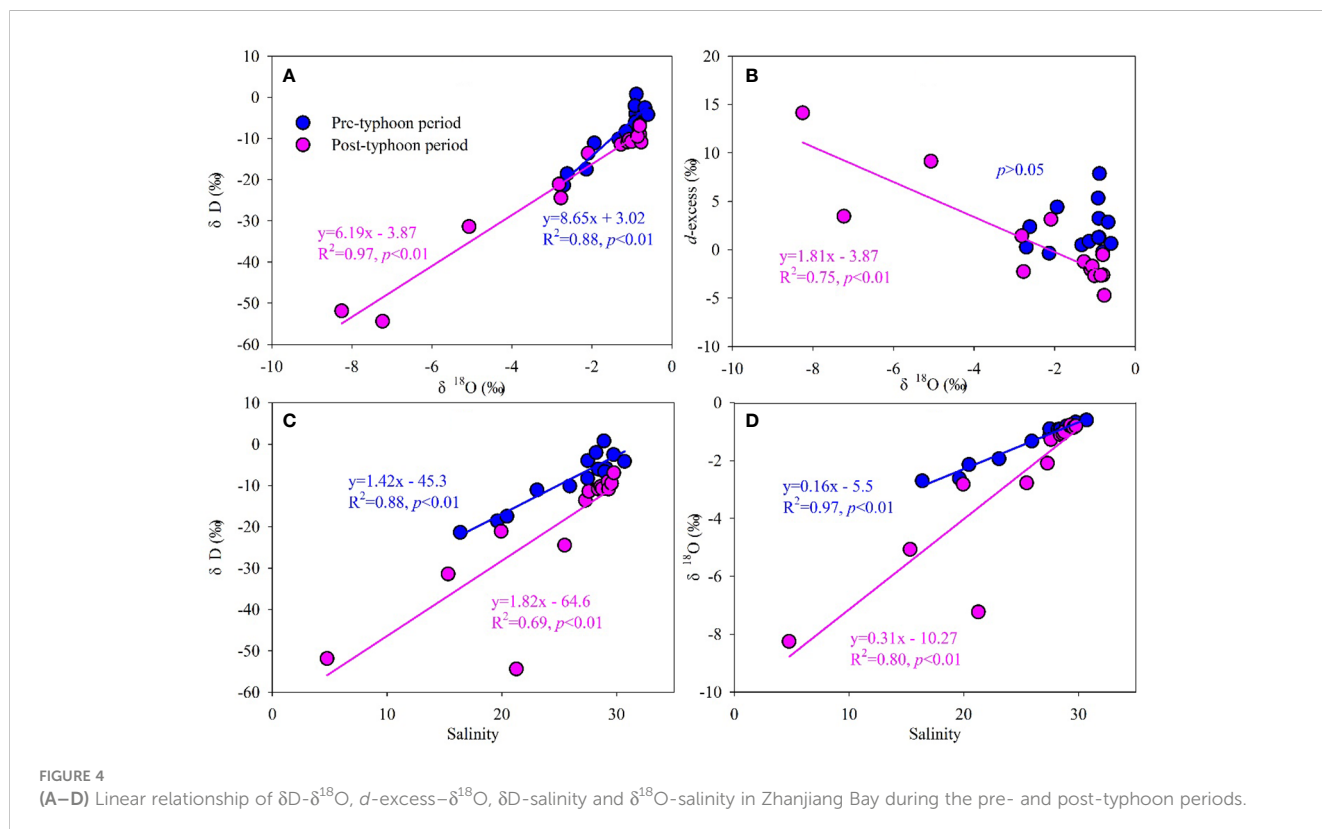
TABLE 3 Variations of temperature (T, °C), salinity, isotopic values (‰) and nutrient concentrations ($\mu\text{mol L}^{-1}$) during the pre- and post-typhoon periods in Zhanjiang Bay.

Periods	Upper bay		Lower bay		Rainwater	
	Pre-typhoon	Post-typhoon	Pre-typhoon	Post-typhoon	Pre-typhoon	Post-typhoon
T	31.35 ± 0.61	29.28 ± 0.58	30.76 ± 0.42	29.54 ± 0.21	-	-
Salinity	23.7 ± 4.5	21.3 ± 8.1	29.2 ± 0.9	29.2 ± 0.4	-	-
δD	-11.3 ± 7.6	-27.4 ± 17.4	-4.6 ± 1.9	-9.6 ± 1.5	-26.6 ± 5.3	-67 ± 25.9
$\delta^{18}\text{O}$	-1.7 ± 0.7	-3.8 ± 2.7	-0.8 ± 0.1	-0.9 ± 0.1	-3.80.5	-9.5 ± 3.2
NO_2^-	3.1 ± 1.2	2.9 ± 1.3	1.3 ± 0.4	0.6 ± 0.2	0.3 ± 0.3	0.2 ± 0.3
NO_3^-	20.6 ± 14.8	35.9 ± 24.6	4.9 ± 2.3	3.4 ± 1.3	34.3 ± 16.4	14.8 ± 15.4
NH_4^+	14.3 ± 4.2	26.9 ± 11.8	7.6 ± 2.7	4.7 ± 0.7	62.6 ± 21.2	26.8 ± 25.3
PO_4^{3-}	2.4 ± 1.0	3.5 ± 1.2	1.0 ± 0.5	1.0 ± 0.3	0.3 ± 0	0.1 ± 0
SiO_3^{2-}	33.5 ± 15.7	42.1 ± 17.3	17.0 ± 4.6	12.9 ± 1.0	0.1 ± 0.1	0.04 ± 0
<i>d</i> -excess	2.4 ± 2.7	3.2 ± 5.8	1.9 ± 2.0	-2.5 ± 1.4	3.8 ± 0.9	9.3 ± 1.1

TABLE 4 Correlation between isotopic values (‰) and temperature (°C), salinity and nutrients (μmol L⁻¹).

	T	S	δD	δ ¹⁸ O	NO ₂ ⁻	NO ₃ ⁻	NH ₄ ⁺	PO ₄ ³⁻	SiO ₃ ²⁻
T	1.00	-0.90**	-0.83**	-0.87**	0.78**	0.83**	0.82**	0.79**	0.81**
S		1.00	0.94**	0.99**	-0.85**	-0.91**	-0.94**	-0.84**	-0.86**
δD			1.00	0.93**	-0.77**	-0.86**	-0.89**	-0.78**	-0.80**
δ ¹⁸ O				1.00	-0.89**	-0.96**	-0.94**	-0.88**	-0.91**
NO ₂ ⁻					1.00	0.96**	0.84**	0.99**	0.97**
NO ₃ ⁻						1.00	0.86**	0.93**	0.99**
NH ₄ ⁺							1.00	0.85**	0.82**
PO ₄ ³⁻								1.00	0.96**
SiO ₃ ²⁻									1.00
T	1.00	0.60*	0.24	0.35	-0.10	-0.32	-0.18	0.02	-0.11
S		1.00	0.83**	0.90**	-0.83**	-0.93**	-0.86**	-0.73**	-0.82**
δD			1.00	0.99**	-0.91**	-0.91**	-0.90**	-0.84**	-0.87**
δ ¹⁸ O				1.00	-0.92**	-0.95**	-0.93**	-0.84**	-0.88**
NO ₂ ⁻					1.00	0.96**	0.99**	0.98**	0.98**
NO ₃ ⁻						1.00	0.97**	0.89**	0.93**
NH ₄ ⁺							1.00	0.96**	0.98**
PO ₄ ³⁻								1.00	0.97**
SiO ₃ ²⁻									1.00

*Correlation is significant at the 0.05 level. **Correlation is significant at the 0.01 level.



summer, the salinity in the lower bay during this period (29.2) was still consistent with the winter (29.2) (Lao et al., 2022b). This indicated the possibility of high-salinity seawater intrusion from the outer bay. In the outer bay, the WGCC affects the Zhanjiang Bay year-round, and the intensity of the coastal current increases in summer (Yang et al., 2003; Xie et al., 2012; Lao et al., 2023d). The WGCC is affected by the subsurface water of the SCS, and its salinity is substantially higher than that of Zhanjiang Bay. This observation is consistent with previous studies (Lao et al., 2022b, 2023c).

During the post-typhoon period, the heavy rainfall and the increase in runoff input could be responsible for the decrease of δD and $\delta^{18}O$ during the post-typhoon period (Figure 2), which is supported by the increase in the slopes of δD -salinity and $\delta^{18}O$ -salinity (Figures 4C, D). Unlike the $\delta D/\delta^{18}O$ -salinity, a decreased slope of δD - $\delta^{18}O$ indicated evaporation or increased intrusion of high-salinity seawater during the typhoon. $\delta^{18}O$ was negatively correlated with d -excess during the post-typhoon period (Figure 4B). However, if evaporation were the primary process for the decreased slope of δD - $\delta^{18}O$, kinetic fractionation caused by evaporation would decrease the d -excess value to $<0\text{‰}$ in the seawater (Lao et al., 2023c). The positive d -excess value (an average of 0.8‰) during the post-typhoon period suggested less influence of evaporation during that period. In addition, the d -excess values from the runoff and oceanic seawater are $\sim 10\text{‰}$ and $\sim 0\text{‰}$, respectively (Kumar et al., 2018; Zhou et al., 2022). A d -excess value of 0.5‰ can be a critical point for indicating water processes, and a value between 0 and this threshold can be considered affected by the mixing with high-salinity seawater, and exceeding this threshold indicates the runoff input (Deshpande et al., 2013). The d -excess value (0.8‰) after the typhoon approaches this threshold, further indicating the impact of high-salinity seawater intrusion. The strong onshore winds caused by typhoons result in residual currents in Zhanjiang Bay flowing from the outer bay to the inner bay (Lao et al., 2023c). This was also supported by decreased nutrient concentrations in the lower bay during the post-typhoon period (Table 2).

The eco-environmental effects of ocean fronts induced the typhoon

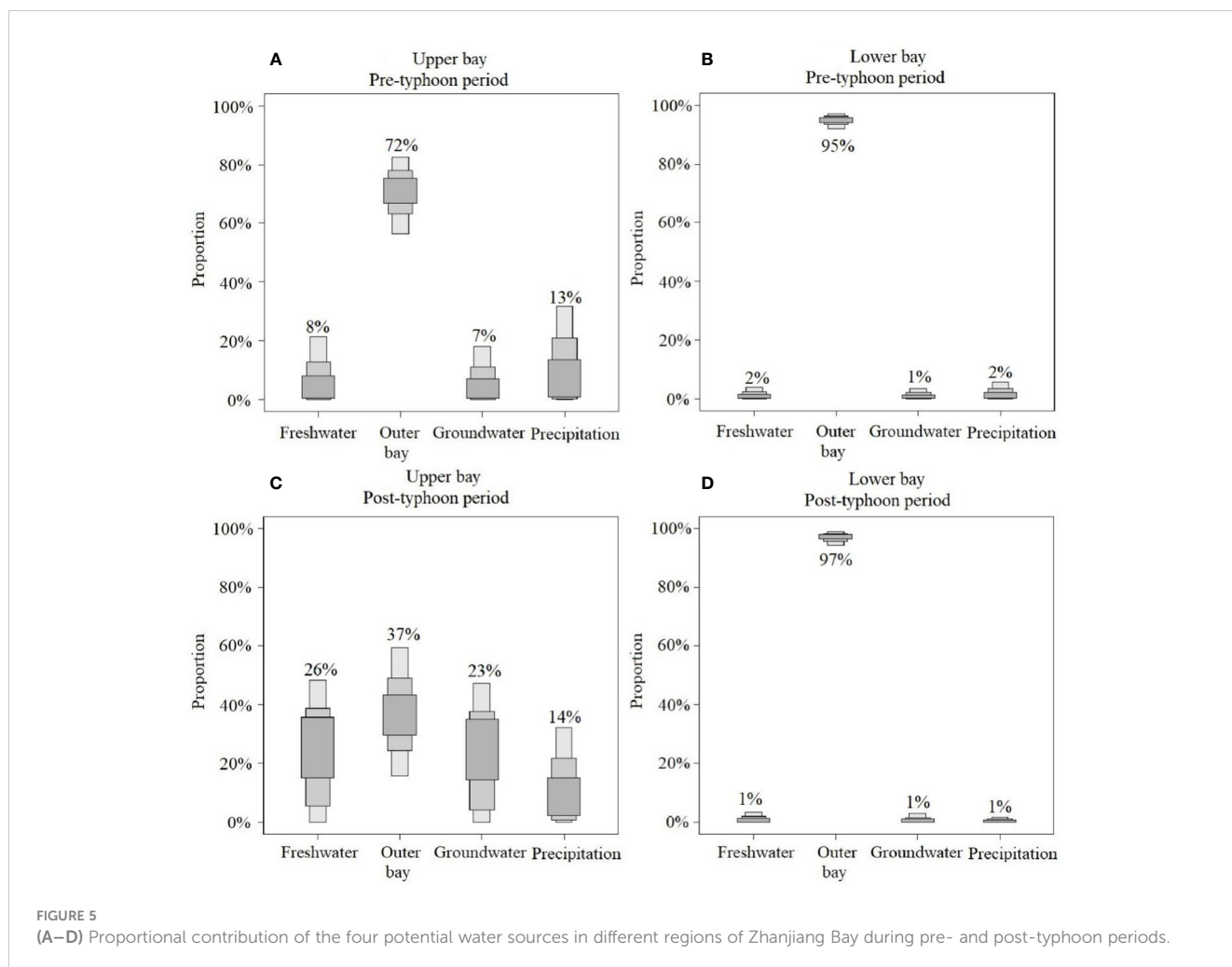
The increase in runoff input during typhoons and the mixing of intruding high-salinity seawater in the bay form a high salinity gradient (strong ocean front). There are two reasons for the relatively small changes in salinity in the lower bay. One is the barrier effect of the front, and the other is the intrusion of high-salinity seawater from the outer bay. Due to the barrier effect of the front, a large amount of fresh water is blocked in the upper bay, resulting in less freshwater flowing into the lower bay. In addition, seawater intrusion into the bay can “buffer” some freshwater input.

Compared to the Typhoon Barijat in 2018 (with a salinity gradient of 0.47 psu km^{-1}) (Lao et al., 2023c), Typhoon Talim formed a much higher salinity gradient in Zhanjiang Bay (1.04 psu km^{-1}), suggesting that a stronger ocean front formed after the Typhoon Talim. The migration trajectory of Typhoon Barijat closely resembles that of Typhoon Talim, with both making direct

landfall in Zhanjiang Bay. Furthermore, the precipitation associated with Typhoon Barijat exhibits a similar pattern to that of Typhoon Talim, both yielding approximately 300 mm (Lao et al., 2023c). This suggests a comparable influx of freshwater into Zhanjiang Bay during these two typhoons. However, the intensity of Typhoon Talim (typhoon level) is stronger than that of Typhoon Barijat (a strong tropical storm), with wind speeds reaching reach 40 m s^{-1} upon landfall, surpassing the maximum speed observed during Typhoon Barijat (28 m s^{-1}). These two typhoons confirmed that that typhoons directly landing in the bay can intrude high-salinity seawater into the bay. However, the stronger Typhoon Talim caused more seawater intrusion and formed a stronger ocean front. This indicates that under the similar typhoon conditions, the strength of the ocean front formation in the bay caused by typhoons depends on the typhoon intensity.

Owing to the lesser influence of kinetic fractionation before and after Typhoon Talim, dual water isotopes can be used to quantify water mixing in Zhanjiang Bay using the Bayesian model. Results were presented in Figure 5. Before the typhoon, the high-salinity water dominated the contribution to the seawater in both the upper and lower bay, and the contribution in the lower bay (95%) was higher than that in the upper bay (72%). The contribution of freshwater in the upper bay (8%) was higher than that in the lower bay (only 2%). This is similar to the results of a previous study in Zhanjiang Bay (Lao et al., 2022b, 2023c). After the typhoon, the contribution of freshwater to the seawater in the upper bay increased remarkably (increased by 18%), while the contribution of high-salinity seawater decreased (decreased by 35%) (Figure 5). In addition, the contribution of groundwater increased to 23% in the upper bay during the post-typhoon period, reflecting massive freshwater input into the upper bay during the typhoon period. During the typhoon period, a significant intrusion of high-salinity seawater into the lower bay was observed, with nearly 97% contribution to the seawater from the outer bay. Moreover, the formation of the ocean front prevented freshwater transport to the lower bay, resulting in a decrease in the contribution of freshwater to the seawater of the lower bay after the typhoon despite heavy rainfall during that period.

Changes in water mixing in Zhanjiang Bay could alter the distribution of nutrients after the typhoon because freshwater can erode substantial terrestrial nutrients into Zhanjiang Bay, while seawater intrusion dilutes the nutrients in the bay. According to the equations (1)-(4), the contribution of each water source to the nutrient loads was quantified, and the results were presented in Figure 6. Before the typhoon, except for NH_4^+ , nutrients in the upper bay mainly originated from the freshwater input (54-65%). The higher contribution to the NH_4^+ loads in the upper bay was observed from the precipitation input, which was similar to a previous study in the northwestern SCS, mainly due to the high NH_4^+ concentration in the atmosphere affected by the industrial activities (Lao et al., 2023b). In the lower bay, the freshwater remained the main contributor to the NO_3^- (50%) during the pre-typhoon period. However, the sources of other nutrients have shifted towards input from the outer bay (69-79%) due to their significant contribution to seawater. Minor nutrient contribution from the groundwater in both upper and lower bay (0-5%). After the



typhoon, the contribution of nutrients has undergone significant changes in Zhanjiang Bay. In the upper bay, the freshwater dominated the contribution of nutrients during the pre-typhoon period (53–95%). The contribution of seawater from the outer bay to the nutrients in this region sharply declined (from 9–41% before the typhoon decreased to 4–15%). The outer bay's seawater dominated the lower bay's nutrient load (54–92%). The contribution of groundwater to the nutrients in Zhanjiang Bay was still minor after the typhoon (Figure 6). Although the typhoon brought heavy rainfall, it also diluted nutrient concentration in the rainwater, resulting in a small contribution of precipitation to the nutrients in Zhanjiang Bay (0–28%). Overall, the formation of the ocean front caused by the typhoon greatly limited nutrient transport between the upper and lower bay. This resulted in nutrient accumulation in the upper bay, while the intrusion of high-salinity seawater diluted the nutrients in the lower bay. Compared to the Typhoon Barijat period (an average of $45.2 \mu\text{mol L}^{-1}$ for DIN) (Lao et al., 2023c), the stronger ocean front induced by the Typhoon Talim resulted in a significant increase in DIN concentration in the upper bay (increased by nearly 50%). This is mainly because runoff is the main DIN source in the bay, and the DIN input exhibited an increasing trend in the recent five years (2017–2021) (He et al., 2023). On the contrary, the input of PO_4^{3-} decreased during this period (He et al., 2023), and thus less change of PO_4^{3-} contribution was observed after the Typhoon Talim compared

to the Typhoon Barijat (an average of $3.5 \mu\text{mol L}^{-1}$ in the upper bay). However, in the lower bay, the DIN concentration during the post-typhoon Talim decreased compared to the Typhoon Barijat (an average of $11.8 \mu\text{mol L}^{-1}$) (Lao et al., 2023c), mainly influenced by more seawater intrusion after stronger typhoon Talim.

Zhanjiang Bay is a region frequently affected by typhoons. Typhoon has caused an increase in the contaminant loads in Zhanjiang Bay, seriously threatening local eco-environment and aquaculture activities and greatly affecting the development of local marine economy and human society (Zhou et al., 2021; Lao et al., 2023c). In addition, due to intense human activities such as dredging and basin dam construction, the intrusion of seawater from the outer bay has increased significantly over the past two decades, which could increase the salinity gradient (frontal enhancement) in the upper bay, thereby retaining more pollutants in the bay (Lao et al., 2022b). Typhoon activities can amplify such ecological risk, especially stronger typhoons (Figure 7). Previous studies have found that after a super typhoon, a large number of land-based pollutants accumulate in Zhanjiang Bay, and the strong degradation of organic matter caused by the typhoon consumes a large amount of oxygen in the water (Zhou et al., 2021). This has caused devastating damage to local aquaculture activities (Zhou et al., 2021). The rainy season is the most frequent period of typhoon activity in Zhanjiang Bay, which is likely an important factor in aggravating eutrophication

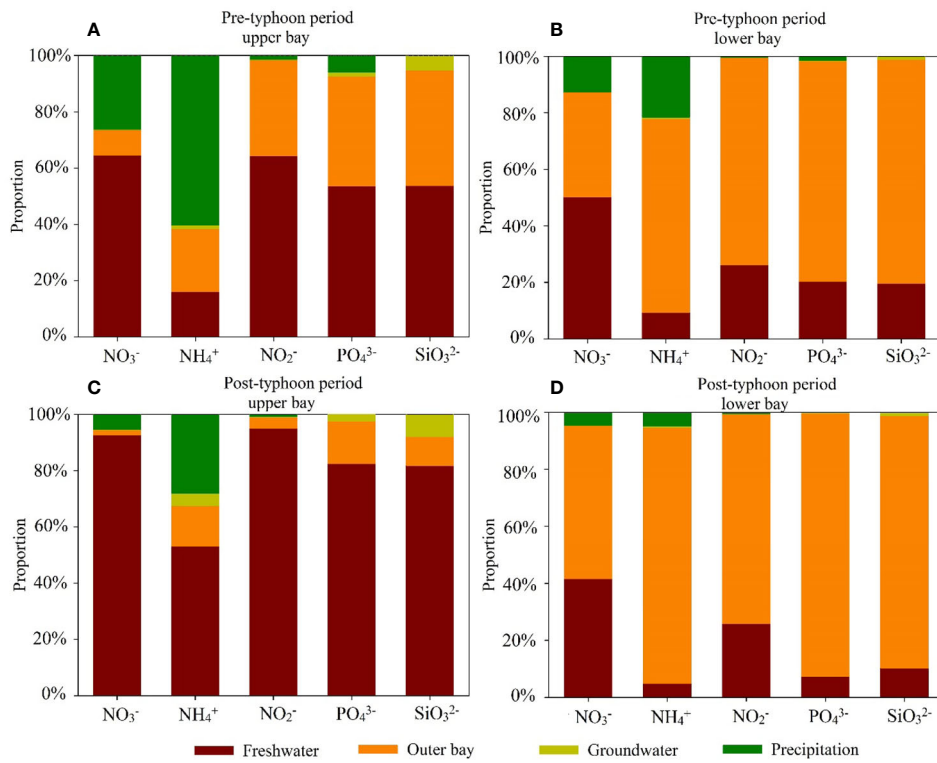


FIGURE 6 (A–D) Proportion of different water sources to the nutrient loads in different regions of Zhanjiang Bay.

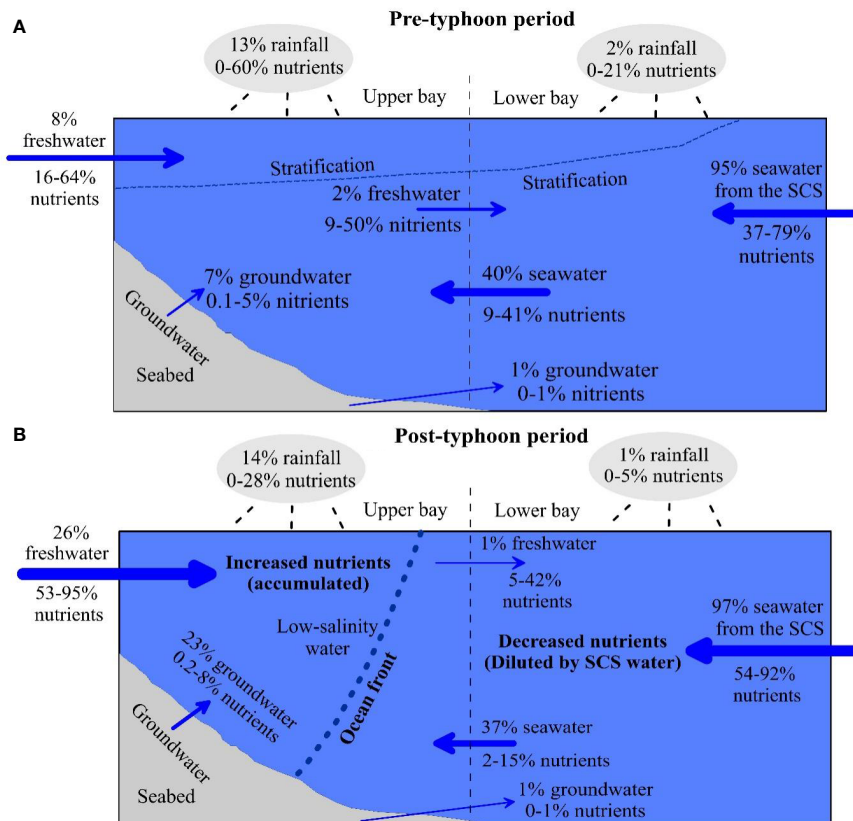


FIGURE 7 (A, B) Conceptual diagram of water mass mixing and nutrient supply in Zhanjiang Bay before and after Typhoon Talim.

(Zhang et al., 2021; Zhang et al., 2022; He et al., 2023). According to historical data, eutrophication in Zhanjiang Bay has shown a significantly increasing trend over three decades, especially during the rainy seasons (He et al., 2023). This has led to an increase in the frequency of harmful algal blooms in Zhanjiang Bay (Zhang et al., 2022), posing a huge threat to the local eco-environment and aquaculture activities. Under global changes, although the number of typhoons may decrease, the intensity of typhoons become stronger (Elsner et al., 2008; Balaguru et al., 2016; Zhou et al., 2019), which may exacerbate the deterioration of water quality in the region. Therefore, the implementation of control measures to control the emission of nutrients into Zhanjiang Bay is urgent.

Conclusion

Two cruises were conducted before and after Typhoon Talim to quantitatively study the changes in hydrodynamics and nutrient supply in the coastal bay caused by the typhoon. Before the typhoon, the water in Zhanjiang Bay experienced strong stratification, resulting in weak water mixing and nutrient exchange within the bay. After the typhoon, a strong external force destroyed the stratification and changed the water mixing in the bay. During the typhoon, in addition to increased runoff freshwater input, strong onshore wind-stress caused massive high-salinity seawater intrusion, which mixed with freshwater to form a strong ocean front in the bay. The strength of the ocean front induced by the typhoon depended on the intensity of typhoons directly landing in Zhanjiang Bay, as stronger typhoons will cause more seawater intrusion from the outer bay. Due to the formation of the ocean front, freshwater and terrestrial nutrients from the upper bay are prevented from being transported to the lower bay (downwards), resulting in a large amount of accumulated pollutants within the bay. On the contrary, due to the impact of high-salinity seawater intrusion, the contribution of seawater from the outer bay has increased and the nutrients in the lower bay area have been diluted. The limitation of this study is that it failed to present the sustained dynamic changes in hydrodynamics and nutrient supply caused by typhoon processes, which is a direction worth further exploration in the future. Nevertheless, this research result will deepen our understanding of the response of the marine ecological environment to ocean hydrodynamic changes caused by typhoons.

References

- Balaguru, K., Foltz, G. R., Leung, L. R., and Emanuel, K. A. (2016). Global warming-induced upper-ocean freshening and the intensification of super typhoons. *Nat. Commun.* 7, 13670. doi: 10.1038/ncomms13670
- Bigg, G. R., and Rohling, E. J. (2000). An oxygen isotope data set for marine waters. *J. Geophys. Res.: Oceans* 105, 8527–8535. doi: 10.1029/2000JC900005
- Brady, E., Stevenson, S., Bailey, D., Liu, Z., Noone, D., Nusbaumer, J., et al. (2019). The connected isotopic water cycle in the Community Earth System Model version 1. *J. Adv. Model. Earth Syst.* 11, 2547–2566. doi: 10.1029/2019MS001663
- Chen, F., Lao, Q., Jia, G., Chen, C., Zhu, Q., and Zhou, X. (2019). Seasonal variations of nitrate dual isotopes in wet deposition in a tropical city in China. *Atmos. Environ.* 196, 1–9. doi: 10.1016/j.atmosenv.2018.09.061
- Chen, D., Lian, E., Shu, Y., Yang, S., Li, Y., Li, C., et al. (2020). Origin of the springtime South China Sea Warm Current in the southwestern Taiwan Strait: Evidence from seawater oxygen isotope. *Sci. China Earth Sci.* 63, 1564–1576. doi: 10.1007/s11430-019-9642-8
- Chen, F., Huang, C., Lao, Q., Zhang, S., Chen, C., Zhou, X., et al. (2021). Typhoon control of precipitation dual isotopes in southern China and its paleoenvironmental implications. *J. Geophys. Res.: Atmos.* 126, e2020JD034336. doi: 10.1029/2020JD034336
- Chen, F., Lao, Q., Lu, X., Wang, C., Chen, C., Liu, S., et al. (2023). A review of the marine biogeochemical response to typhoons. *Mar. pollut. Bull.* 194, 115408. doi: 10.1016/j.marpolbul.2023.115408
- Chen, C., Lao, Q., Zhou, X., Jin, G., Zhu, Q., and Chen, F. (2024). Tracks of typhoon movement (left and right sides) control marine dynamics and eco-environment in the

Data availability statement

The raw data supporting the conclusions of this article will be made available by the authors, without undue reservation.

Author contributions

CC: Investigation, Methodology, Writing – original draft, Writing – review & editing. QL: Methodology, Validation, Visualization, Writing – original draft, Writing – review & editing. XZ: Data curation, Formal Analysis, Methodology, Writing – review & editing. QZ: Methodology, Writing – review & editing. FC: Conceptualization, Funding acquisition, Project administration, Writing – review & editing.

Funding

The author(s) declare financial support was received for the research, authorship, and/or publication of this article. This study was supported by the National Natural Science Foundation of China (42276047, 92158201), Entrepreneurship Project of Shantou (2021112176541391), Scientific Research Start-Up Foundation of Shantou University (NTF20006), Guangdong Provincial College Innovation Team Project (2019KCXTF021).

Conflict of interest

The authors declare that the research was conducted in the absence of any commercial or financial relationships that could be construed as a potential conflict of interest.

Publisher's note

All claims expressed in this article are solely those of the authors and do not necessarily represent those of their affiliated organizations, or those of the publisher, the editors and the reviewers. Any product that may be evaluated in this article, or claim that may be made by its manufacturer, is not guaranteed or endorsed by the publisher.

- coastal bays after typhoons: A case study in Zhanjiang Bay. *Sci. Total Environ.* 912, 168944. doi: 10.1016/j.scitotenv.2023.168944
- Craig, H. (1961). Isotopic variations in meteoric waters. *Science* 133, 1702–1703. doi: 10.1126/science.133.3465.1702
- Craig, H., and Gordon, L. I. (1965). “Deuterium and oxygen 18 variations in the ocean and the marine atmosphere,” in *Stable Isotopes in Oceanographic Studies and Paleotemperatures*. Ed. E. Tongiorgi (Consiglio Naz. delle Ric., Lab. di Geol. Nucl., Pisa, Italy), 9–130.
- Dansgaard, W. (1964). Stable isotopes in precipitation. *Tellus* 16, 436–468. doi: 10.1111/tus.1964.16.issue-4
- Dawson, T. E., and Siegwolf, R. T. (2007). Using stable isotopes as indicators, tracers, and recorders of ecological change: some context and background. *Terrestrial Ecol.* 1, 1–18. doi: 10.1016/S1936-7961(07)01001-9
- Deshpande, R. D., Muraleedharan, P. M., Singh, R. L., Kumar, B., Rao, M. S., Dave, M., et al. (2013). Spatio-temporal distributions of $\delta^{18}\text{O}$, δD and salinity in the Arabian Sea: identifying processes and controls. *Mar. Chem.* 157, 144–161. doi: 10.1016/j.marchem.2013.10.001
- Doong, D. J., Peng, J. P., and Babanin, A. V. (2019). Field investigations of coastal sea surface temperature drop after typhoon passages. *Earth Syst. Sci. Data* 11, 323–340. doi: 10.5194/essd-11-323-2019
- Elsner, J. B., Kossin, J. P., and Jagger, T. H. (2008). The increasing intensity of the strongest tropical cyclones. *Nature* 455, 92–95. doi: 10.1038/nature07234
- Feng, J., Li, D., Dang, W., and Zhao, L. (2023). Changes in storm surges based on a bias-adjusted reconstruction dataset from 1900 to 2010. *J. Hydrol.* 617, 128759. doi: 10.1016/j.jhydrol.2022.128759
- He, G., Lao, Q., Jin, G., Zhu, Q., and Chen, F. (2023). Increasing eutrophication driven by the increase of phosphate discharge in a subtropical bay in the past 30 years. *Front. Mar. Sci.* 10, 1184421. doi: 10.3389/fmars.2023.1184421
- Jiang, T., Wu, G., Niu, P., Cui, Z., Bian, X., Xie, Y., et al. (2022). Short-term changes in algal blooms and phytoplankton community after the passage of Super Typhoon Lekima in a temperate and inner sea (Bohai Sea) in China. *Ecotoxicol. Environ. Saf.* 232, 113223. doi: 10.1016/j.ecoenv.2022.113223
- Kumar, P. K., Singh, A., and Ramesh, R. (2018). Controls on $\delta^{18}\text{O}$, δD and $\delta^{18}\text{O}$ -salinity relationship in the northern Indian Ocean. *Mar. Chem.* 207, 55–62. doi: 10.1016/j.marchem.2018.10.010
- Lao, Q., Chen, F., Jin, G., Lu, X., Chen, C., Zhou, X., et al. (2023a). Characteristics and mechanisms of typhoon-induced decomposition of organic matter and its implication for climate change. *J. Geophys. Res.: Biogeosci.* 128, e2023JG007518. doi: 10.1029/2023JG007518
- Lao, Q., Liu, S., Ling, Z., Jin, G., Chen, F., Chen, C., et al. (2023d). External dynamic mechanisms controlling the periodic offshore blooms in Beibu Gulf. *J. Geophys. Res.: Oceans* 128, e2023JC019689. doi: 10.1029/2023JC019689
- Lao, Q., Lu, X., Chen, F., Chen, C., Jin, G., and Zhu, Q. (2023c). A comparative study on source of water masses and nutrient supply in Zhanjiang Bay during the normal summer, rainstorm, and typhoon periods: Insights from dual water isotopes. *Sci. Total Environ.* 903, 166853. doi: 10.1016/j.scitotenv.2023.166853
- Lao, Q., Lu, X., Chen, F., Jin, G., Chen, C., Zhou, X., et al. (2023b). Effects of upwelling and runoff on water mass mixing and nutrient supply induced by typhoons: Insight from dual water isotopes tracing. *Limnol. Oceanogr.* 68, 284–295. doi: 10.1002/lno.12266
- Lao, Q., Wu, J., Chen, F., Zhou, X., Li, Z., Chen, C., et al. (2022b). Increasing intrusion of high salinity water alters the mariculture activities in Zhanjiang Bay during the past two decades identified by dual water isotopes. *J. Environ. Manage.* 320, 115815. doi: 10.1016/j.jenvman.2022.115815
- Lao, Q., Zhang, S., Li, Z., Chen, F., Zhou, X., Jin, G., et al. (2022a). Quantification of the seasonal intrusion of water masses and their impact on nutrients in the Beibu Gulf using dual water isotopes. *J. Geophys. Res.: Oceans* 127, e2021JC018065. doi: 10.1029/2021JC018065
- Li, D., Chen, J., Ni, X., Wang, K., Zeng, D., Wang, B., et al. (2019). Hypoxic bottom waters as a carbon source to atmosphere during a typhoon passage over the East China Sea. *Geophys. Res. Lett.* 46, 11329–11337. doi: 10.1029/2019GL083933
- Li, Y., Yang, D., Xu, L., Gao, G., He, Z., Cui, X., et al. (2022). Three types of typhoon-induced upwellings enhance coastal algal blooms: A case study. *J. Geophys. Res.: Oceans* 127, e2022JC018448. doi: 10.1029/2022JC018448
- Lian, E., Yang, S., Wu, H., Yang, C., Li, C., and Liu, J. T. (2016). Kuroshio subsurface water feeds the wintertime Taiwan Warm Current on the inner East China Sea shelf. *J. Geophys. Res.: Oceans* 121, 4790–4803. doi: 10.1002/2016JC011869
- Liu, S. S., Sun, L., Wu, Q., and Yang, Y. J. (2017). The responses of cyclonic and anticyclonic eddies to typhoon forcing: The vertical temperature-salinity structure changes associated with the horizontal convergence/divergence. *J. Geophys. Res.: Oceans* 122, 4974–4989. doi: 10.1002/2017JC012814
- Lu, X., Zhou, X., Jin, G., Chen, F., Zhang, S., Li, Z., and Lao, Q. (2022). Biological impact of Typhoon Wipha in the coastal area of western Guangdong: A comparative field observation perspective. *Journal of Geophysical Research: Biogeosciences*. 127(2), e2021JG006589. doi: 10.1029/2021JG006589
- Meng, Q., Zhou, F., Ma, X., Xuan, J., Zhang, H., Wang, S., et al. (2022). Response process of coastal hypoxia to a passing typhoon in the East China Sea. *Front. Mar. Sci.* 9, 892797. doi: 10.3389/fmars.2022.892797
- Moore, J. W., and Semmens, B. X. (2008). Incorporating uncertainty and prior information into stable isotope mixing models. *Ecol. Lett.* 11, 470–480. doi: 10.1111/j.1461-0248.2008.01163.x
- Mori, N., Kato, M., Kim, S., Mase, H., Shibutani, Y., Takemi, T., et al. (2014). Local amplification of storm surge by Super Typhoon Haiyan in Leyte Gulf. *Geophys. Res. Lett.* 41, 5106–5113. doi: 10.1002/2014GL060689
- Oshun, J., Dietrich, W. E., Dawson, T. E., and Fung, I. (2016). Dynamic, structured heterogeneity of water isotopes inside hillslopes. *Water Resour. Res.* 52, 164–189. doi: 10.1002/2015WR017485
- Price, J. F. (1981). Upper ocean response to a hurricane. *J. Phys. Oceanogr.* 11, 153–175. doi: 10.1175/1520-0485(1981)011<0153:UORTAH>2.0.CO;2
- Qiu, D., Zhong, Y., Chen, Y., Tan, Y., Song, X., and Huang, L. (2019). Short-term phytoplankton dynamics during typhoon season in and near the Pearl River Estuary, South China Sea. *J. Geophys. Res.: Biogeosci.* 124, 274–292. doi: 10.1029/2018JG004672
- Reyes-Macaya, D., Hoogakker, B., Martínez-Méndez, G., Llanillo, P. J., Grasse, P., Mohtadi, M., et al. (2022). Isotopic characterization of water masses in the Southeast Pacific region: Paleooceanographic implications. *J. Geophys. Res.: Oceans* 127, e2021JC017525. doi: 10.1029/2021JC017525
- Rohling, E. J. (2007). Progress in paleosalinity: overview and presentation of a new approach. *Paleoceanography* 22, PA3215. doi: 10.1029/2007PA001437
- Sengupta, S., Parekh, A., Chakraborty, S., Ravi Kumar, K., and Bose, T. (2013). Vertical variation of oxygen isotope in Bay of Bengal and its relationships with water masses. *J. Geophys. Res.: Oceans* 118, 6411–6424. doi: 10.1002/2013JC008973
- Shibano, R., Yamanaka, Y., Okada, N., Chuda, T., Suzuki, S. I., Niino, H., et al. (2011). Responses of marine ecosystem to typhoon passages in the western subtropical North Pacific. *Geophys. Res. Lett.* 38, L18608. doi: 10.1029/2011GL048717
- Tanim, A. H., and Goharian, E. (2021). Developing a hybrid modeling and multivariate analysis framework for storm surge and runoff interactions in urban coastal flooding. *J. Hydrol.* 595, 125670. doi: 10.1016/j.jhydrol.2020.125670
- Wang, B., Chen, J., Jin, H., Li, H., Huang, D., and Cai, W. J. (2017). Diatom bloom-derived bottom water hypoxia off the Changjiang estuary, with and without typhoon influence. *Limnol. Oceanogr.* 62, 1552–1569. doi: 10.1002/lno.10517
- Wang, X., Wang, W., and Tong, C. (2016). A review on impact of typhoons and hurricanes on coastal wetland ecosystems. *Acta Ecol. Sin.* 36, 23–29. doi: 10.1016/j.chnaes.2015.12.006
- Wu, J., Lao, Q., Chen, F., Huang, C., Zhang, S., Wang, C., et al. (2021). Water mass processes between the South China Sea and the western Pacific through the Luzon Strait: insights from hydrogen and oxygen isotopes. *J. Geophys. Res.: Oceans* 126, e2021JC017484. doi: 10.1029/2021JC017484
- Xie, L. L., Cao, R. X., and Shang, Q. T. (2012). Process of study on coastal circulation near the shore of western Guangdong. *J. Guangdong Ocean Univ.* 32, 94–98.
- Yang, S., Bao, X., Chen, C., and Chen, F. (2003). Analysis on characteristics and mechanism of current system in west coast of Guangdong Province in the summer. *Acta Oceanol. Sin.* 25, 1–8.
- Zhang, P., Peng, C., Zhang, J., Zhang, J., Chen, J., and Zhao, H. (2022). Long-term harmful algal blooms and nutrients patterns affected by climate change and anthropogenic pressures in the Zhanjiang Bay, China. *Front. Mar. Sci.* 9, 849819. doi: 10.3389/fmars.2022.849819
- Zhang, J., Zhang, Y., Zhang, P., Li, Y., Li, J., Luo, X., et al. (2021). Seasonal phosphorus variation in coastal water affected by the land-based sources input in the eutrophic Zhanjiang Bay, China. *Estuar. Coast. Shelf Sci.* 252, 107277. doi: 10.1016/j.ecss.2021.107277
- Zhao, Y., Uthaiyan, K., Lu, Z., Li, Y., Liu, J., Liu, H., et al. (2021). Destruction and reinstatement of coastal hypoxia in the South China Sea off the Pearl River estuary. *Biogeosciences* 18, 2755–2775. doi: 10.5194/bg-18-2755-2021
- Zhou, X., Jin, G., Li, J., Song, Z., Zhang, S., Chen, C., et al. (2021). Effects of Typhoon Mujigae on the biogeochemistry and ecology of a semi-enclosed bay in the northern South China Sea. *J. Geophys. Res.: Biogeosci.* 126, e2020JG006031. doi: 10.1029/2020JG006031
- Zhou, X., Liu, Z., Yan, Q., Zhang, X., Yi, L., Yang, W., et al. (2019). Enhanced tropical cyclone intensity in the western North Pacific during warm periods over the last two millennia. *Geophys. Res. Lett.* 46, 9145–9153. doi: 10.1029/2019GL083504
- Zhou, F., Wu, J., Chen, F., Chen, C., Zhu, Q., Lao, Q., et al. (2022). Using stable isotopes ($\delta^{18}\text{O}$ and δD) to study the dynamics of upwelling and other oceanic processes in northwestern South China Sea. *J. Geophys. Res.: Oceans* 127, e2021JC017972. doi: 10.1029/2021JC017972